

RESEARCH ARTICLE

Optimal Design of the Cascade Controller for Reheating Furnace by Taguchi Method

CHIEN-JUNG CHEN^{ID}, YU-CHENG LIAO^{ID}, AND FU-I CHOU^{ID}

Department of Electrical Engineering, National Kaohsiung University of Science and Technology, Kaohsiung 80778, Taiwan

Corresponding author: Fu-I Chou (ryan.chou.0110.1111@nkust.edu.tw)

ABSTRACT Reheating furnaces are used to uniformly heat billets (blooms, billets, or slabs) to between 1000°C and 1300°C before hot rolling. Cascade control is widely used in temperature controllers of the reheating furnace. Unfortunately, the relationship between temperature indicator controllers (TIC) and flow indicator controllers (FIC) usually changes with a single slope. It means that temperature load disturbances cannot be effectively resolved. In this study, the relationship between TIC and FIC is proposed to be nonlinear with multiple slopes, which is used to accelerate the temperature response and increase the temperature stability under high or low load conditions. The temperature controller parameters are more diverse, so this study optimizes the temperature controller parameters and determines the characteristic curves between TIC and FIC effectively and quickly by using the Taguchi method. The performance of the multi-slope method and the single-slope method is evaluated in an actual heating furnace. The experimental results show that the proposed method in this study improves the mean square error and standard deviation by 33.76% and 22.44%, respectively. After commissioning, the parameter combination (including the characteristic curve) has a remarkable performance in the heating zone, which can be used to reduce temperature disturbance, accelerate the temperature response, and increase temperature stability in the reheating furnace.

INDEX TERMS Taguchi method, combustion system, cascade control, furnace hearth temperature controller.

I. INTRODUCTION

Hot rolling production line is a manufacturing process in which metal materials such as steel and aluminum are heated to a high temperature and then passed through a series of rollers to shape and form them into desired shapes and sizes. The high temperature and pressure applied during hot rolling help to reduce the thickness of the metal and improve its overall mechanical properties, making it more suitable for various industrial applications [1]. Hot rolling production lines typically consist of multiple stages, including reheating furnaces, roughing mills, finishing mills, and cooling beds [2]. These production lines require precise control of temperature, pressure, and rolling speed to ensure consistent and high-quality output.

A reheating furnace is ascribed to upstream equipment in the steel rolling line. It is used to heat the stock temperature

and satisfy the rolling process requirement. A typical continuous reheating furnace consists of three zones: the preheating zone, the heating zone, and the soaking zone, respectively [3]. The heat convection design of the heating furnace allows hot gases to flow from the equalization zone to the preheating zone so that there can be no burner in the preheating zone, shown in Figure 1. The heating zone is used to heat the steel billet to a temperature ranging from 1000°C to 1200°C, while the soaking zone is employed to uniformly heat the steel billet to a temperature between 1100°C and 1300°C [4].

Directly measuring the surface temperature of steel billets inside the furnace chamber is nearly impossible. Therefore, temperature control refers to regulating the local temperature measured by thermocouples within the combustion system of the furnace rather than controlling the temperature of the steel billets.

There are various methods for temperature control, including manual control, fuzzy control, and PI/PID single-loop control [5], [6]. Cascade control is the most common and

The associate editor coordinating the review of this manuscript and approving it for publication was Sawyer Duane Campbell^{ID}.

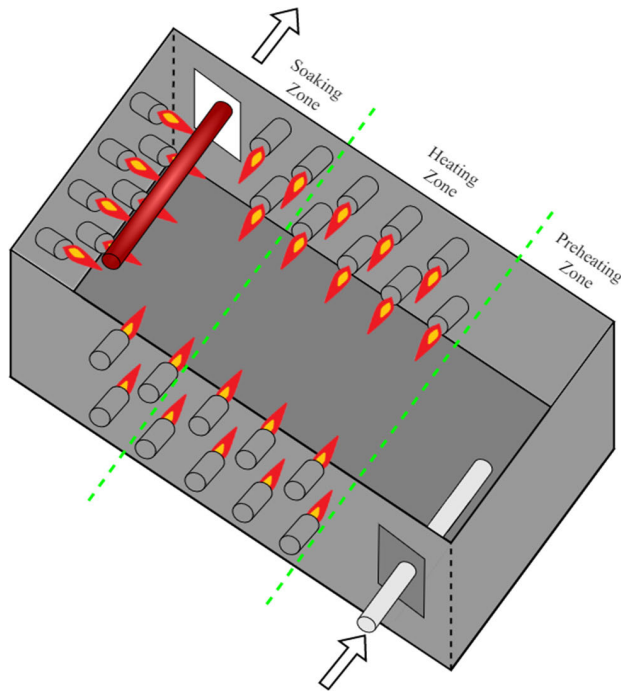


FIGURE 1. Typical bird view of a reheating furnace.

widely applied in heating furnaces. Cascade control consists of two control loops: the primary control loop and the secondary control loop [7]. The output of the primary control loop is used to determine the setpoint for the secondary control loop. One of the main functions of cascade control is to eliminate load disturbance variations before the system's output loses its ability to closely follow the setpoint.

For temperature control, the temperature indicating controller (i.e., TIC) serves as the primary controller for temperature regulation, while the flow indicating controller (i.e., FIC) serves as the secondary controller for flow control. However, when the TIC sets the flow rate for the FIC, the change is often made with a single slope. This means that the slope of the FIC flow rate setting change is the same regardless of whether the temperature changes at low or high loads. Therefore, this study proposes optimizing the setting of the FIC flow rate change slope using the characteristic curve of the temperature controller. An appropriate characteristic curve can provide different slopes of fuel flow under various temperature load conditions, thereby addressing disturbances caused by load variations. Furthermore, since changes in the slope also affect parameters such as the gain and integral time of the TIC, it is necessary to include parameter optimization in the process. Adjusting parameters of the on-site process affects the stability of temperature control. Prolonged or repeated use of inappropriate parameters can also influence fuel consumption and the quality of steel billets, potentially impacting factory operations. Therefore, using a full factorial experiment to find the optimal parameters is time-consuming and only allows for discussing the best combination of these values. Another

issue of concern is how to obtain combinations of parameter values using an effective and efficient method.

The Taguchi Method is characterized by a comprehensive and efficient experimental design approach, enabling the identification of optimal parameter combinations with a relatively small number of experiments. It simultaneously takes into account the stability and robustness of the system. This study is based on the Taguchi method to determine characteristic curves of the temperature controller and adjust the slope, gain, and integral time parameters of the cascade control. This paper introduces the proposed temperature control method for combustion systems and demonstrates its performance. Integrating multiple slopes and parameter optimization strategies can alleviate temperature control disturbances and accelerate response times. Parameter adjustments were conducted on the temperature controller of the on-site heating furnace, and the temperature control performance of single-slope and multi-slope strategies was compared. The results indicate that the method outperforms typical single-slope cascade controllers regarding temperature stability.

The remainder of the paper is organized as follows. Section II surveys the techniques of temperature control and optimal solution. Section III describes a method for optimizing cascade control parameters based on the Taguchi method. Section IV presents the experimental results and analysis. Finally, conclusions are given in Section V.

II. RELATED WORK

This section reviews recent research on temperature control and parameter optimization. Reference [8] proposes a cascade fuzzy PID (C-Fuzzy-PID) complex control method to regulate the outer ring temperature and inner ring fuel flow. Using Levinson's prediction combined with fuzzy PID to control the inner ring fuel flow not only overcomes the large inertia of the fuel supply and the effect of transmission lag temperature response but also suppresses temperature variations, disturbances, and other factors. The proposed control algorithm is proved to be robust and adaptable to the temperature control of high-speed airflow wind tunnel (HAWT). Reference [9] proposes a cascaded control scheme combining Levinson prediction with fuzzy PID control for fuel flow and Smith prediction with fuzzy PID control for airflow to achieve precise gas temperature control. Experimental results demonstrate that the proposed algorithm can achieve fast, stable, and non-overshooting gas temperature control on the Supersonic Hot Gas Test System (SHSTS) simulation testbed. The control accuracy can reach $\pm 5^\circ\text{C}$.

Reference [10] proposes the Fuzzy logic Taguchi method (FLTM) for optimizing the parameters of the wire bonding process. This process has 5 parameters with 3 levels for each parameter and 243 parameter combinations. Only 27 experiments are required to obtain the optimized parameters using Taguchi method. This study shows that the proposed FLTM provides the characteristics of smaller ball size and larger ball shear in the wire bonding process. In reference [11], gated

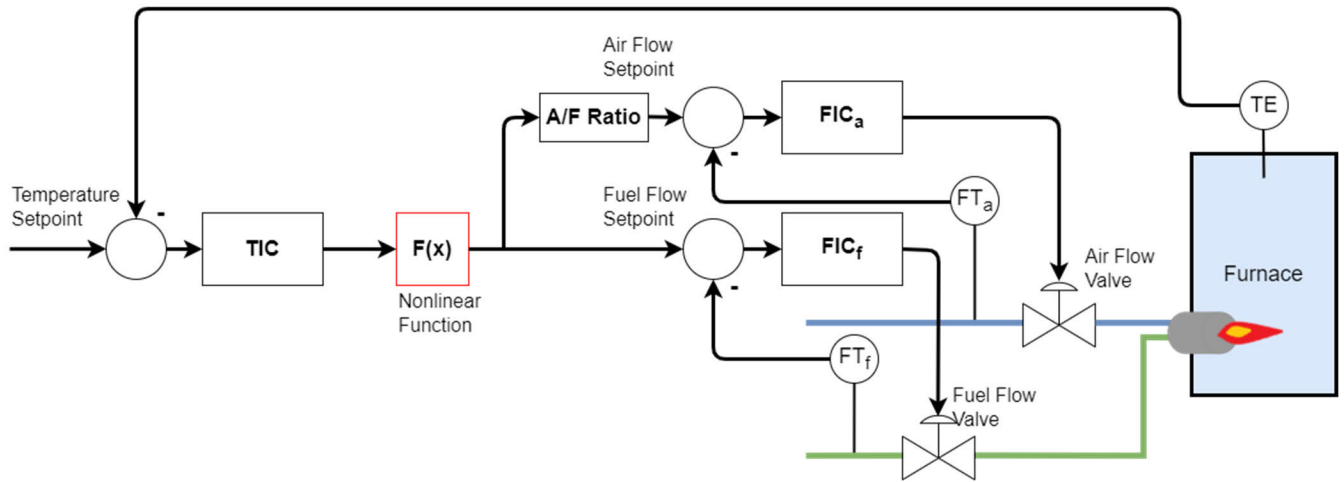


FIGURE 2. The configuration of the proposed cascade control system.

recurrent unit (GRU) is predicted Dissolved Oxygen Concentration (DOC) in aquaculture water, aiming to enhance the efficiency of aquaculture production. This study employs the Taguchi method to optimize hyperparameters, including the number of hidden layer neurons, iterations, batch size, learning rate, and dropout rate.

Experiments demonstrate that the proposed method improves the accuracy of GRU predictions for DOC, effectively increasing the survival rate of cultured fish. In reference [12], the optimization of parameters for a tapping center machine is achieved by integrating uniform design, Adaptive Neuro-Fuzzy Inference System (ANFIS), and Multi-Objective Particle Swarm Optimizer (MOPSO). An ANFIS model is constructed using synchronization errors and cycle time, and then the MOPSO algorithm is employed to search for the optimal parameter combination for two ANFIS models. Experimental results demonstrate that this method can shorten processing time, reduce synchronization errors, and improve production output.

III. PROPOSED METHOD

A. TAGUCHI METHOD

The Taguchi method is used to design a robust process or product that is less sensitive to variation caused by external factors. Its main feature is the optimization of process or product parameters with minimal experimental cost in order to achieve the goal of quality improvement. The two main tools of the Taguchi method are the orthogonal arrays (OA) and the signal-to-noise ratio (SNR) [13], [14], [15].

Select the appropriate OA based on the number of control factors and levels. The most important feature of an OA is that any two rows are orthogonal, meaning that the frequency of occurrence of each control factor level is the same. Table 1 is an L_4 OA used for three control factors, each with two levels, for a total of four experiments. An OA matrix arranges numbers in rows and columns, each representing a specific

TABLE 1. Orthogonal array (L_4).

L_4	Factors		
	A	B	C
1	1	1	2
2	1	2	1
3	2	1	1
4	2	2	2

factor and each expressing the combination of factor levels used in each experimental run.

SNR is used to verify the robustness of the design, and determine the best combination of control factor values. SNR can be divided into three types: smaller-the-better, larger-the-better, and nominal-is-best. These three types can be evaluated as:

$$\eta_i = -10 \log \left(\frac{1}{n} \sum_{j=1}^n y_{ij}^2 \right) \quad (1)$$

$$\eta_i = -10 \log \left(\frac{1}{n} \sum_{j=1}^n \frac{1}{y_{ij}^2} \right) \quad (2)$$

$$\eta_i = -10 \log \left(\frac{1}{n} \sum_{j=1}^n y_{ij}^2 - m_{ij}^2 \right) \quad (3)$$

where η_i is the objective function, y_{ij} is the experimental output value of the i^{th} row of OA, m_{ij} is the target value of the i^{th} row of OA, and n is the number of trials. A higher η_i indicates better performance, and besides, chooses the appropriate type based on the nature of the problem.

The response table can be constructed based on the experimental results' SNR. The response table facilitates an intuitive understanding of the impact of different factor levels on the experimental outcomes and aids in selecting the optimal parameter combination to achieve the goal of parameter optimization. Suppose the optimized parameters' experimental results are worse than the combinations from

the orthogonal array. In that case, it is necessary to reconsider whether other factors are not considered or the factor levels are inappropriate.

B. CASCADE CONTROL

Cascade control is a typical control system used for temperature control; it's widely used in the combustion system of reheating furnaces. The characteristic of cascade control is its ability to rapidly and effectively overcome disturbances entering the secondary loop. Due to the cascade control with the secondary control loop, it can rapidly mitigate disturbances within the inner loop, thereby enhancing the efficiency of the control loop [16], [17], [18], [19]. It is suitable for controlled processes with larger time constants and pure lag, such as power plants [16], Steel plants [17], and so on.

The configuration of the proposed cascade control system is shown in Fig. 2. TIC is the primary controller, FIC_f and FIC_a are secondary controllers, TE is the measured temperature of the furnace hearth, FT_f is the measured fuel flow, and FT_a is the measured air flow. These controllers (including primary and secondary) are all PID controllers. In this study, the manipulated variable of the outer loop main controller (TIC) is transformed through the characteristic curve of the temperature controller to provide a setpoint for the inner loop secondary controller (FIC_f). It is also given as a setpoint to the inner loop secondary controller (FIC_a), passing through the air/fuel ratio (A/F ratio) at the same time [20], [21].

The typical relationship between the manipulated variable of TIC and the setpoint of FIC is linear. It means that regardless of the load conditions, a single slope is used for the variation of FIC setpoints. Therefore, this study proposes a non-linear relationship between the manipulated variable of TIC and the setpoint of FIC, as the multi-slope relationship provides different slopes for the variation of FIC setpoints under different load conditions.

This study uses the Taguchi method to determine the optimal parameters of the temperature controller. The correspondence between the manipulated variable (MV) of the temperature controller and the setpoint (SP) of the fuel flow controller is expressed as Eq (4) and Fig. 3.

$$y = \begin{cases} \frac{A_i - 0}{40 - 0} (x - 0), & \text{for } 0\% \leq x \leq 40\% \\ \frac{B_j - A_i}{70 - 40} (x - 40), & \text{for } 40\% < x \leq 70\% \\ \frac{100 - B_j}{100 - 70} (x - 70), & \text{for } x > 70\% \end{cases} \quad (4)$$

where y is the percent of fuel flow, x is the percent of TIC MV, A_i is the point1 of the characteristic curve in Fig. 3, B_j is the point2 of the characteristic curve in Fig. 3.

According to empirical rules, TIC is divided into three different slopes: below 40%, 40% to 70%, and above 70%. According to empirical rules, TIC is divided into three different slopes: below 40%, 40% to 70%, and above 70%. The ranges 0 to A_i (point1) determine the slope below 40%, A_i

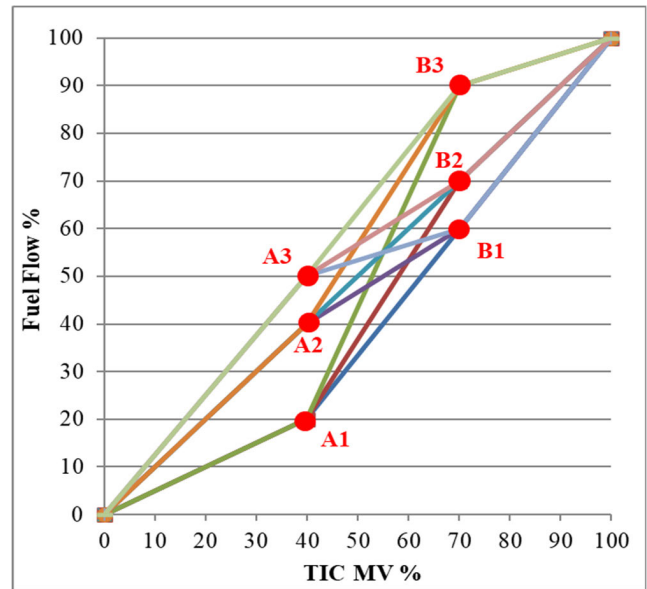


FIGURE 3. The characteristic curve of the temperature controller.

(point1) to B_j (point2) determine the slope between 40% and 70%, and B_j (point2) to 100 determine the slope above 70%. In total, there are 9 combinations of characteristic curves. Among them, the typical characteristic curve is the one represented by A2 and B2.

IV. EXPERIMENTS AND RESULT ANALYSIS

This study found the most suitable parameter combination by using Taguchi method. Next, we compare parameter combinations before and after commissioning. The experimental process was carried out at a steel factory in Tainan, Taiwan.



FIGURE 4. Charge side of reheating furnace.

A. DATA AND ENVIRONMENT

The reheating furnace used in the experimental implementation employs the SIEMENS CPU416 as the controller for combustion control. There is no burner in the preheating zone of the reheating furnace, which relies solely on thermal convection to transport hot gases from the heating and soaking zones to the preheating zone. Therefore, this study doesn't discuss the preheating zone in this paper. The drawing of the section view of the reheating furnace was shown in Fig. 5. Each zone can be divided into top and bottom zones; therefore, this study targeted four zones for parameter optimization, namely heating zone 1 (heating zone top), heating zone 2 (heating zone bottom), soaking zone 3 (soaking zone top) and soaking zone 4 (soaking zone bottom). Each zone has two thermocouples, and the process value for the TIC is obtained by taking the maximum value of the two thermocouples, recorded every second.

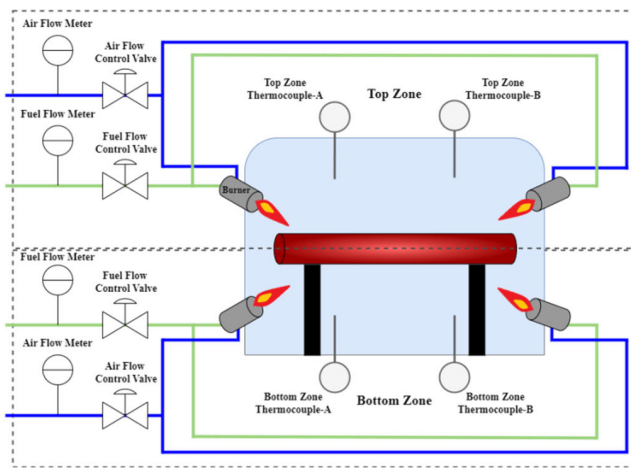


FIGURE 5. Section view of reheating furnace of each zone.

B. OPTIMAL RESULTS

This research plan proposes to optimize the parameters of the temperature controller using the Taguchi method. These parameters include the relationship between the output of the temperature controller and the fuel flow rate, as well as the Gain and Integral Time of the temperature controller. The original temperature controller parameters were point 1 of the curve (factor A) of 40 and point 2 of the curve (factor B) of 70 for each zone. Moreover, the parameters of heating zone 1, heating zone 2, soaking zone 3, and soaking zone 4 were respectively 0.06, 0.06, 0.01, and 0.01 in proportional gain (factor C) and 30, 40, 25, and 30 in integral time (factor D). At the same time, the Level 2 parameters are currently used in the original process. In other words, A2B2C2D2 are each zone's original temperature controller parameters. The parameters and levels of the temperature controller for each zone are shown in Table 2. The three levels of point 1 of the curve (factor A) were 20, 40, and 50, and those of point 2 (factor B) were 55, 70, and 90. The three levels of proportional gain (factor C) were 0.04, 0.06, and

0.08, and those of integral time (factor D) were 20, 30, and 40 in heating zone 1. The three levels of proportional gain (factor C) were 0.04, 0.06, and 0.08, and those of integral time (factor D) were 30, 40, and 50 in heating zone 2. The three levels of proportional gain (factor C) were 0.05, 0.1, and 0.2, and those of integral time (factor D) were 15, 25, and 35 in soaking zone 3. The three levels of proportional gain (factor C) were 0.05, 0.1, and 0.2, and those of integral time (factor D) were 20, 30, and 40 in soaking zone 4. Instead of 81 experiments, the $L_9(4^3)$ OA required only 9 experiments.

Many statistical indicators are used to determine the performance of the parameters [2], [22], [23]. This study evaluated the performance of the parameters by using the mean square error (*MSE*), the mean absolute error (*MAE*), and the standard deviation (*SD*).

MSE, *MAE*, and *SD* can be evaluated as:

$$MSE = \frac{1}{n} \sum_{i=1}^n (T_SP_i - T_PV_i)^2 \tag{5}$$

$$MAE = \frac{1}{n} \sum_{i=1}^n |T_SP_i - T_PV_i| \tag{6}$$

$$T_PV = \frac{1}{N} \sum_{i=1}^N T_PV_i$$

$$SD = \sqrt{\frac{1}{N} \sum_{i=1}^n (T_PV_i - T_PV)^2} \tag{7}$$

where T_SP_i is the setpoint of the temperature control, T_PV_i is the process variable of the temperature control. When the *MSE*, *MAE*, and *SD* value verges on 0, the performance of this parameter combination is outstanding.

TABLE 2. Parameters and levels of the temperature controller.

Zone	Factor	Level		
		1	2	3
Heating Zone1	A: Point 1 of the curve	20%	40%	50%
	B: Point 2 of the curve	55%	70%	90%
	C: Proportional Gain	0.04	0.06	0.08
	D: Integral Time	20	30	40
Heating Zone2	A: Point 1 of the curve	20%	40%	50%
	B: Point 2 of the curve	55%	70%	90%
	C: Proportional Gain	0.04	0.06	0.08
	D: Integral Time	30	40	50
Soaking Zone3	A: Point 1 of the curve	20%	40%	50%
	B: Point 2 of the curve	55%	70%	90%
	C: Proportional Gain	0.005	0.01	0.02
	D: Integral Time	15	25	35
Soaking Zone4	A: Point 1 of the curve	20%	40%	50%
	B: Point 2 of the curve	55%	70%	90%
	C: Proportional Gain	0.005	0.01	0.03
	D: Integral Time	20	30	40

The optimization experiments were conducted in July 2023. During the continuous production process with the same set point of temperature, data was collected continuously for 60 minutes, with data recorded every second. Eq (5) was used to evaluate the performance of the L_9 parameters for the four zones. Next, the *MSE* was converted by using SNR,

which has the higher-the-better characteristic. The experimental results for each zone are shown in Table 3 to Table 6. Table 3 shows that factor levels 1, 1, 3, and 2 were selected for factors A, B, C, and D, respectively. Thus, the best factor-level combinations for the temperature controller in heating zone 1 were A1: 20 (%), B1: 55 (%), C3: 0.08, and D2: 30. The optimal characteristic curve is the one represented by A1 and B1 in Fig.3. Fig. 6 plots the effects of the factors on the temperature controller in heating zone 1; the most important factors were factors A and B.

TABLE 3. Experimental parameters and results for heating zone 1 in L_9 .

No	A	B	C	D	MSE
1	1	1	1	1	13.5
2	1	2	2	2	11.6
3	1	3	3	3	16.3
4	2	1	2	3	11.9
5	2	2	3	1	22.6
6	2	3	1	2	6.68
7	3	1	3	2	8.62
8	3	2	1	3	19.8
9	3	3	2	1	23.1
Level1	-22.0	-22.22	-24.8	-24.97	
Level2	-25.0	-24.76	-25.93	-24.06	
Level3	-27.24	-27.26	-23.5	-25.21	
Optimal	1	1	3	2	

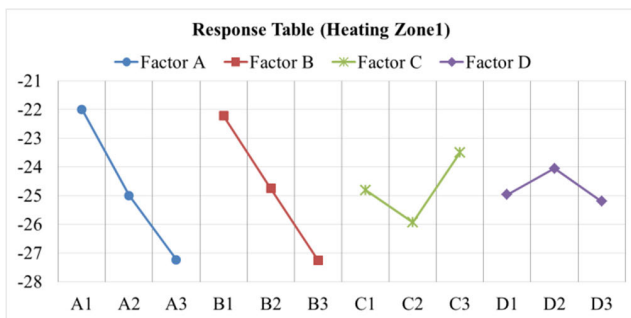


FIGURE 6. Plots of factor effects on heating zone 1.

Table 4 shows that factor levels 1, 2, 3, and 2 were selected for factors A, B, C, and D, respectively. Thus, the best factor-level combinations for the temperature controller in heating zone 2 were A1: 20 (%), B2: 70 (%), C3: 0.08, and D2: 40. The optimal characteristic curve is the one represented by A1 and B2 in Fig.3. Fig. 7 plots the effects of the factors on the temperature controller in heating zone 2; the most important factor was factors D.

TABLE 4. Experimental parameters and results for heating zone 2 in L_9 .

No	A	B	C	D	MSE
1	1	1	1	1	35.5
2	1	2	2	2	3.13
3	1	3	3	3	8.93
4	2	1	2	3	7.28
5	2	2	3	1	17.3
6	2	3	1	2	1.29
7	3	1	3	2	5.77
8	3	2	1	3	4.49
9	3	3	2	1	4.05
Level1	-18.94	-23.39	-20.56	-25.21	
Level2	-21.43	-17.13	-23.11	-14.54	
Level3	-21.33	-21.18	-18.03	-21.95	
Optimal	1	2	3	2	

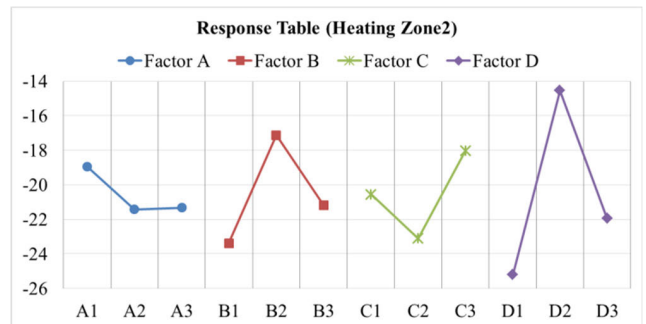


FIGURE 7. Plots of factor effects on heating zone 2.

Table 5 shows that factor levels 1, 1, 2, and 2 were selected for factors A, B, C, and D, respectively. Thus, the best factor-level combinations for the temperature controller in soaking zone 3 were A1: 20 (%), B1: 55 (%), C2: 0.01, and D2: 25. The optimal characteristic curve is the one represented by A1 and B1 in Fig.3. Fig. 8 plots the effects of the factors on the temperature controller in soaking zone 3; the most important factor was factors C. Table 6 shows that factor levels 1, 1, 2, and 1 were selected for factors A, B, C, and D, respectively. Thus, the best factor-level combinations for the temperature controller in soaking zone 3 were A1: 20 (%), B1: 55 (%), C2: 0.01, and D1: 20. The optimal characteristic curve is the one represented by A1 and B1 in Fig.3. Fig. 9 plots the effects of the factors on the temperature controller in soaking zone 4; the most important factor was factors B.

The optimal parameter combinations for each zone are different, but the factor A for each zone is consistently 1

TABLE 5. Experimental parameters and results for soaking zone 3 in L_9 .

No	A	B	C	D	MSE
1	1	1	1	1	5.61
2	1	2	2	2	2.24
3	1	3	3	3	114
4	2	1	2	3	4.26
5	2	2	3	1	7.76
6	2	3	1	2	4.45
7	3	1	3	2	22.4
8	3	2	1	3	8.74
9	3	3	2	1	38.2
Level1	-25.19	-19.29	-20.69	-27.53	
Level2	-25.93	-24.82	-17.86	-19.51	
Level3	-27.02	-34.02	-39.58	-31.09	
Optimal	1	1	2	2	

TABLE 6. Experimental parameters and results for soaking zone 4 in L_9 .

No	A	B	C	D	MSE
1	1	1	1	1	2.74
2	1	2	2	2	1.18
3	1	3	3	3	1.91
4	2	1	2	3	2.86
5	2	2	3	1	2.42
6	2	3	1	2	1.17
7	3	1	3	2	1.65
8	3	2	1	3	2.75
9	3	3	2	1	3.33
Level1	-8.09	-6.95	-9.02	-7.84	
Level2	-9.45	-9.02	-8.25	-8.52	
Level3	-8.46	-10.03	-8.75	-9.64	
Optimal	1	1	2	1	

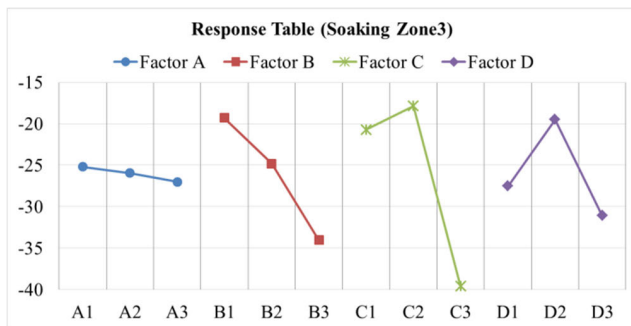


FIGURE 8. Plots of factor effects on soaking zone 3.

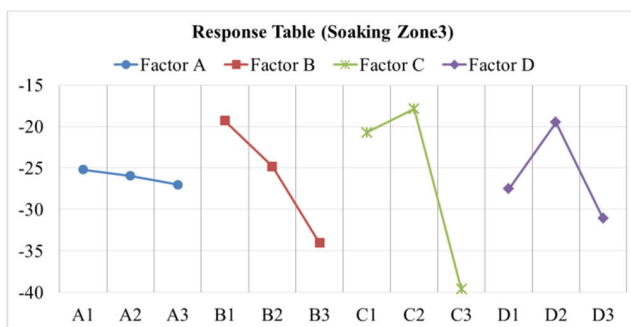


FIGURE 9. Plots of factor effects on soaking zone 4.

(20%). Increasing the slope can improve the performance of the temperature controller under conditions with a load above 40%.

C. EXPERIMENTAL VALIDATION

In the validation step, this study compared the performance of optimal parameters with the original parameters for each

zone. For heating zone 1, the optimal parameters were A1, B1, C3, and D2, and it was compared with the original parameters A2, B2, C2, and D2. For heating zone 2, the optimal parameters were A1, B2, C3, and D2, and it was compared with the original parameters A2, B2, C2, and D2. For Soaking zone 3, the optimal parameters were A1, B1, C2, and D2, and it was compared with the original parameters A2, B2, C2, and D2. For Soaking zone 4, the optimal parameters were A1, B1, C2, and D1, and it was compared with the original parameters A2, B2, C2, and D2.

There are many variables in the reheating furnace, so it's impossible to have the same situation in the test.

The validation situation is described as

- 1) The steel type was 303.
- 2) Slab Temperature before entry of reheating furnace is 300°C.
- 3) The set point of heating zone 1 and heating zone 2, before and after parameter adjustment, is 1200°C.
- 4) The set point of soaking zone 3 and soaking zone 4, before and after parameter adjustment, is 1280°C.
- 5) Running times and production of the before and after commissioning were 1 hour and 52 tons, respectively.

Fig. 10 presents the control effectiveness before and after commissioning for each zone. The TIC_PV (Before commissioning) means that the temperature controller uses the original parameters, and the TIC_PV (After commissioning) means that the temperature controller uses the optimized parameters. The results show that the process temperature of TIC_PV (After commissioning) is closer to the setpoint temperature. Since the temperature rise of the steel billet in the heating zone has an extensive range (300°C ~ 1200°C),

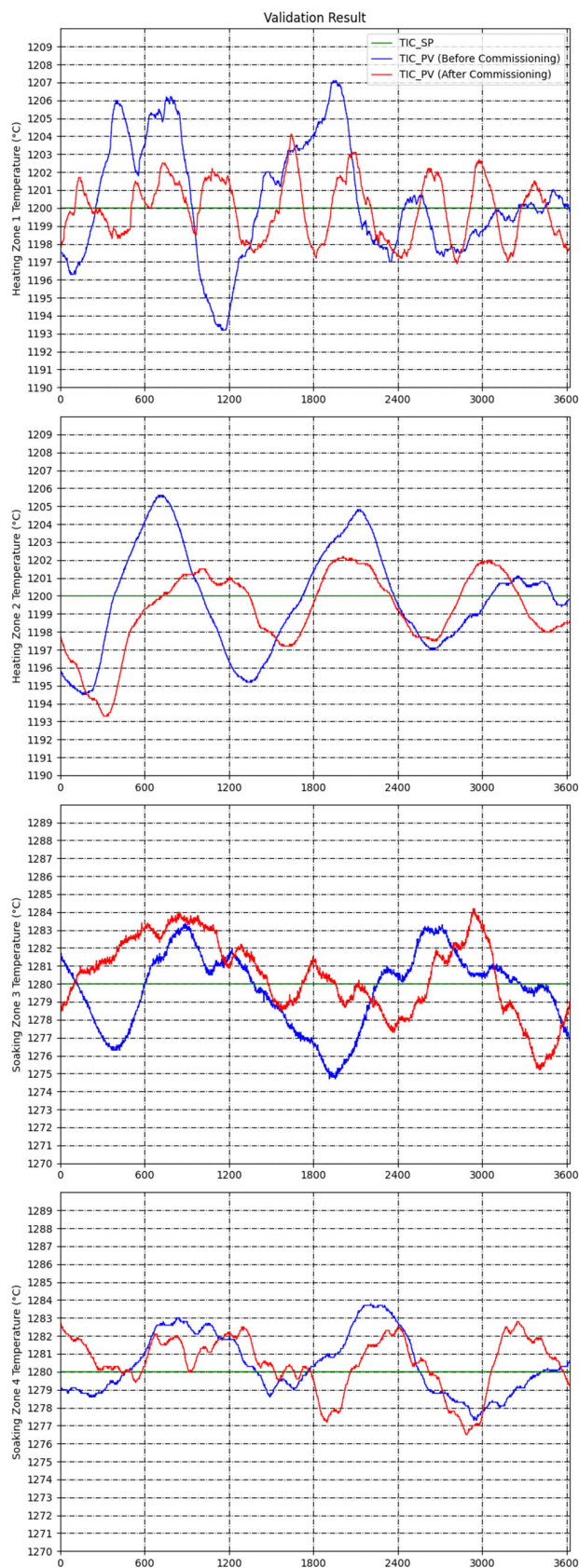


FIGURE 10. Validation Compare.

TABLE 7. Validation result.

Zones	Before commissioning			After commissioning		
	MSE	MAE	SD	MSE	MAE	SD
Heating 1	10.71	2.60	3.25	2.76	1.44	1.66
Heating 2	8.64	2.41	2.93	5.30	1.80	2.15
Soaking 3	4.80	1.76	2.15	4.65	1.82	2.11
Soaking 4	3.05	1.43	1.70	2.47	1.29	1.49

it can be regarded as an influential change in temperature loading. Therefore, TIC_PV (After commissioning) has a better performance in the heating zone.

However, the temperature rise range of the steel billet in the soaking zone is small (1200~1280), which can be regarded as the temperature loading variation is slight. Therefore, the performance difference between TIC_PV (After commissioning) and TIC_PV (Before commissioning) in the soaking zone is insignificant.

In order to further compare the parameter combination performance before and after commissioning, the mean absolute error (MAE) and standard deviation (SD) are added as evaluation indicators at this stage. The closer the process variable is to the setpoint in temperature control, the higher the stability. When MSE, MAE, and SD values are more relative to 0, it indicates better performance in temperature control. The parameter combination After commissioning exhibited lower MSE, MAE, and SD values in the heating zone 1 & 2 and soaking zone 4, whereas the lower MSE and SD values in the soaking zone 3. A lower MSE indicates a more minor hunting error, signifying that the temperature control strategy is more capable of providing stability. In heating zone 1, the MSE for the controller before and after commissioning is 10.71 and 2.76, respectively. The MAE for the same controllers is 2.60 and 1.44, and the SD is 3.25 and 1.66. In heating zone 2, the MSE for the controller before and after commissioning is 8.64 and 5.30, respectively. The MAE is 2.41 and 1.80, and the SD is 2.93 and 2.15. In soaking zone 3, the MSE for the controller before and after commissioning is 4.80 and 4.65, respectively. The MAE is 1.76 and 1.82, and the SD is 2.15 and 2.11. In soaking zone 4, the MSE for the controller before and after commissioning is 3.05 and 2.47, respectively. The MAE is 1.43 and 1.29, and the SD is 1.70 and 1.49. It means that the parameter combination After commissioning has more effective control over temperature. The above values are listed in Table 5. Although the parameter combination after commissioning has only slightly improved the soaking zones 3 and the soaking zone 4, it has obvious improvements in the heating zones 1 and the heating zone 2.

V. CONCLUSION

This study proposes changing the relationship between TIC MV and FIC SP to a non-linear one, providing different

FIC SP ramp rates for various load conditions. Additionally, the optimization of four parameters is carried out and compared with the original parameters by using the Taguchi method. Experimental results show that increasing the slope for loads above 40% and optimizing the temperature controller parameters with the Taguchi method can enhance temperature control stability, overcome disturbances caused by load variations, and simultaneously improve the efficiency of the heating furnace and rolling mill production line.

Different steel grades, like SS-304 and SS-316, have distinct material properties. Therefore, the characteristic curve determined for SS-303 may not be optimized for other steel types, implicating a multi-objective issue. In the future, our research team will also explore multi-objective approaches.

REFERENCES

- [1] P. Skopec, T. Vyhldal, and J. Knobloch, "Reheating furnace modeling and temperature estimation based on model order reduction," in *Proc. 22nd Int. Conf. Process Control (PC19)*, Strbske Pleso, Slovakia, Jun. 2019, pp. 55–61, doi: [10.1109/PC.2019.8815053](https://doi.org/10.1109/PC.2019.8815053).
- [2] Y. Yang, J. Kroeze, and M. Reuter, "Simulation of slab movement and transient heating in a continuous steel reheat furnace," *Prog. Comput. Fluid Dyn.*, vol. 4, 2004, doi: [10.1504/PCFD.2004.003785](https://doi.org/10.1504/PCFD.2004.003785).
- [3] S. M. Zanoli, C. Pepe, E. Moscoloni, and G. Astolfi, "Data analysis and modelling of billets features in steel industry," *Sensors*, vol. 22, no. 19, p. 7333, Sep. 2022, doi: [10.3390/s22197333](https://doi.org/10.3390/s22197333).
- [4] Z. Yang and X. Luo, "Parallel numerical calculation on GPU for the 3-dimensional mathematical model in the walking beam reheating furnace," *IEEE Access*, vol. 7, pp. 44583–44595, 2019, doi: [10.1109/ACCESS.2019.2908522](https://doi.org/10.1109/ACCESS.2019.2908522).
- [5] D. Zhenhai and S. Lianyun, "Design of temperature controller for heating furnace in oil field," *Phys. Proc.*, vol. 24, pp. 2083–2088, 2012, doi: [10.1016/j.phpro.2012.02.305](https://doi.org/10.1016/j.phpro.2012.02.305).
- [6] C.-J. Chen, F.-I. Chou, and J.-H. Chou, "Temperature prediction for reheating furnace by gated recurrent unit approach," *IEEE Access*, vol. 10, pp. 33362–33369, 2022, doi: [10.1109/ACCESS.2022.3162424](https://doi.org/10.1109/ACCESS.2022.3162424).
- [7] T. R. Biyanto, M. S. Alfarisi, N. Afdanny, H. Setiawan, and A. Hasan, "Simultaneous optimization of tuning PID cascade control system using duelist algorithms," in *Proc. Int. Seminar Intell. Technol. Appl. (ISITIA)*, Lombok, Indonesia, Jul. 2016, pp. 601–606, doi: [10.1109/ISITIA.2016.7828728](https://doi.org/10.1109/ISITIA.2016.7828728).
- [8] Y. Li, C. Cai, K.-M. Lee, and F. Teng, "A novel cascade temperature control system for a high-speed heat-airflow wind tunnel," *IEEE/ASME Trans. Mechatronics*, vol. 18, no. 4, pp. 1310–1319, Aug. 2013, doi: [10.1109/TMECH.2013.2262077](https://doi.org/10.1109/TMECH.2013.2262077).
- [9] C. Cai, L. Guo, Q. Ma, and Y. Yang, "Gas temperature control of a supersonic heat-airflow simulated test system," *IEEE Access*, vol. 8, pp. 101093–101103, 2020, doi: [10.1109/ACCESS.2020.2998458](https://doi.org/10.1109/ACCESS.2020.2998458).
- [10] J.-T. Tsai, C.-C. Chang, W.-P. Chen, and J.-H. Chou, "Optimal parameter design for IC wire bonding process by using fuzzy logic and Taguchi method," *IEEE Access*, vol. 4, pp. 3034–3045, 2016, doi: [10.1109/ACCESS.2016.2581258](https://doi.org/10.1109/ACCESS.2016.2581258).
- [11] P.-Y. Yang, Y.-C. Liao, and F.-I. Chou, "Artificial intelligence in Internet of Things system for predicting water quality in aquaculture fishponds," *Comput. Syst. Sci. Eng.*, vol. 46, no. 3, pp. 2861–2880, 2023, doi: [10.32604/csse.2023.036810](https://doi.org/10.32604/csse.2023.036810).
- [12] P.-Y. Chang, F.-I. Chou, P.-Y. Yang, and S.-H. Chen, "Hybrid multi-object optimization method for tapping center machines," *Intell. Autom. Soft Comput.*, vol. 36, no. 1, pp. 23–38, 2023, doi: [10.32604/iasec.2023.031609](https://doi.org/10.32604/iasec.2023.031609).
- [13] G. Taguchi, S. Chowdhury, and S. Taguchi, *Robust Engineering*. New York, NY, USA: McGraw-Hill, 2000.
- [14] H. H. Lee, *Taguchi Methods: Principles and Practices of Quality Design*. Taiwan: Gau-Lih, 2011.
- [15] D. C. Montgomery, *Design and Analysis of Experiments*. Hoboken, NJ, USA: Wiley, 2009.
- [16] C. Huang, Y. Bai, and X. Liu, "H-infinity state feedback control for a class of networked cascade control systems with uncertain delay," *IEEE Trans. Ind. Informat.*, vol. 6, no. 1, pp. 62–72, Feb. 2010, doi: [10.1109/TII.2009.2033589](https://doi.org/10.1109/TII.2009.2033589).
- [17] Z. Fan, Z. Ren, and A. Chen, "A modified cascade control strategy for tobacco re-drying moisture control process with large delay-time," *IEEE Access*, vol. 8, pp. 2145–2152, 2020, doi: [10.1109/ACCESS.2019.2960192](https://doi.org/10.1109/ACCESS.2019.2960192).
- [18] S. Song, L. Xie, and W.-J. Cai, "Auto-tuning of cascade control systems," in *Proc. 4th World Congr. Intell. Control Automat.*, Shanghai, China, vol. 4, 2002, pp. 3339–3343, doi: [10.1109/WCICA.2002.1020152](https://doi.org/10.1109/WCICA.2002.1020152).
- [19] I. Kaya, N. Tan, and D. P. Atherton, "Improved cascade control structure and controller design," in *Proc. 44th IEEE Conf. Decis. Control*, Seville, Spain, 2005, pp. 3055–3060, doi: [10.1109/CDC.2005.1582630](https://doi.org/10.1109/CDC.2005.1582630).
- [20] L. Xiaohua, W. Yashuai, and L. Yunhai, "Research on the intelligent temperature control based on ANFIS for reheating furnace in rolling steel line," in *Proc. 27th Chin. Control Decis. Conf. (CCDC)*, Qingdao, China, May 2015, pp. 5688–5692.
- [21] L. Zenghuan, H. Guangxiang, and W. Lizhen, "Optimization of furnace combustion control system based on double cross-limiting strategy," in *Proc. Int. Conf. Intell. Comput. Technol. Autom.*, Changsha, China, May 2010, pp. 858–861.
- [22] L. Lin, C.-Y. Chen, H.-Y. Yang, Z. Xu, and S.-H. Fang, "Dynamic system approach for improved PM2.5 prediction in Taiwan," *IEEE Access*, vol. 8, pp. 210910–210921, 2020.
- [23] S. Sha, J. Li, K. Zhang, Z. Yang, Z. Wei, X. Li, and X. Zhu, "RNN-based subway passenger flow rolling prediction," *IEEE Access*, vol. 8, pp. 15232–15240, 2020.



CHIEN-JUNG CHEN received the B.S. degree from the Department of Information Technology and Management, Shih Chien University, Taiwan, in 2010, and the M.S. degree from the Department of Electrical Engineering, National University of Kaohsiung, Taiwan, in 2012. He is currently pursuing the Ph.D. degree with the National Kaohsiung University of Science and Technology, Kaohsiung, Taiwan. His research interests include fuzzy systems, evolutionary algorithms, image processing, and neural networks.



YU-CHENG LIAO received the B.S. degree in computer and communication from Shu-Te University, Kaohsiung, Taiwan, in 2019, and the M.S. degree in electrical engineering from the National Kaohsiung University of Science and Technology, Kaohsiung, in 2021, where he is currently pursuing the Ph.D. degree. His research interests include artificial intelligence applications, evolutionary algorithms, machine learning, and quality engineering.



FU-I CHOU received the B.S. degree in electrical engineering from the National University of Kaohsiung, Taiwan, in 2010, the M.S. degree in electrical engineering from the National Dong Hwa University, Taiwan, in 2012, and the Ph.D. degree in electrical engineering from the National Cheng-Kung University, Taiwan, in 2019. From August 2019 to January 2020, he was an Assistant Professor with the National Chin-Yi University of Technology, Taiwan. He was a Deputy Engineer with the Metal Industries Research and Development Centre, Taiwan, from September 2012 to August 2019. He is currently an Assistant Professor with the Department of Automation Engineering, National Formosa University, Taiwan. His research interests include state observer design, automation and control, industrial robotics, artificial intelligence applications, machine learning, quality engineering, evolutionary optimization, and machine vision. He received the 2019 Doctoral Dissertation Award from the Chinese Automatic Control Society, Taiwan. He and his colleagues proposed the research and development achievement, Intelligent 3-D Visual Automation for Shoes Roughing and Cementing Equipment, received the 2019 American Edison Bronze Award in robot field, and the Sixth National Industry Innovation Award from the Taiwan Ministry of Economics.